Probing Interfacial Water on Nanodiamonds in Colloidal Dispersion

ARTICLE *in* JOURNAL OF PHYSICAL CHEMISTRY LETTERS · AUGUST 2015

Impact Factor: 7.46 · DOI: 10.1021/acs.jpclett.5b00820 · Source: PubMed

THE JOURNAL OF PHYSICAL CHEMISTRY Letters

Letter

pubs.acs.org/JPCL

Probing Interfacial Water on Nanodiamonds in Colloidal Dispersion

Tristan Petit,*[,†] Hayato Yuzawa,[‡] Masanari Nagasaka,[‡] Ryoko Yamanoi,[§] Eiji Osawa,[§] Nobuhiro Kosugi,[‡] and Emad F. Aziz[†,‡,∥]

[†]Institute of Methods for Materials Development, Helmholtz-Zentrum Berlin, Albert-Einstein-Strasse 15, 12489 Berlin, Germany

[‡]Institute for Molecular Science, Myodaiji, Okazaki 444-8585, Japan

[§]Nanocarbon Research Institute, Shinshu University, Ueda, Nagano 386-8567, Japan

[∥]Freie Universität Berlin, FB Physik, Arnimallee 14, 14195 Berlin, Germany

Supporting Information

ABSTRACT: The structure of interfacial water layers around nanoparticles dispersed in an aqueous environment may have a significant impact on their reactivity and on their interaction with biological species. Using transmission soft X-ray absorption spectroscopy in liquid, we demonstrate that the unoccupied electronic states of oxygen atoms from water molecules in aqueous colloidal dispersions of nanodiamonds have a different signature than bulk water. X-ray absorption spectroscopy can thus probe interfacial water molecules in colloidal dispersions. The impacts of nanodiamond surface chemistry and concentration on interfacial water electronic signature are discussed.

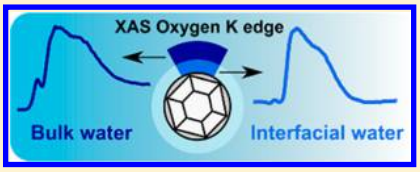

The organization of water molecules close to solid surfaces[1−3] or around proteins[4,5] differs significantly from pure water. Structured water may impact protein recognition[2,6] but is also believed to affect electrochemical and catalytic reactions at interfaces.[7,8] Reorganization of solvent molecules is likely to occur around colloidal nanoparticles[9] and its understanding is of outermost importance to better estimate their reactivity and interaction with biological moieties in aqueous environment. Nevertheless, the structure of solvent molecules around nanomaterials in colloidal dispersion remains largely unexplored.[9−11]

Nanodiamonds (NDs) are of particular interest for the investigation of interfacial water since the existence of an ordered water shell ranging from 2 to 4 water layers was recently suggested.[11,12] The interfacial water layer may play an essential role in the colloidal stability of small NDs,[13] in their photoluminescence[14] or in the enhancement of magnetic resonance imaging signal from Gd-functionalized NDs,[15] but its structure is still unknown. Unusual water adsorption on dry NDs have already been characterized by infrared spectroscopy[16] and differential scanning calorimetry.[12,17] Recently, interfacial water layers around NDs were probed directly in aqueous solution by interferometry[11] and Raman spectroscopy[14] but provided limited information about its molecular and electronic structure.

X-ray Absorption Spectroscopy (XAS) and X-ray Emission Spectroscopy (XES) at the oxygen K edge, probing respectively the unoccupied and occupied electronic states through the excitation of a core electron, were extensively applied to characterize the solvation shells of ionic species in aqueous solutions because these methods are sensitive to the hydrogen bonds network of water.[18−24] Recently, Total Electron Yield (TEY) XAS measurements of gold electrode−water interface demonstrated that interfacial water have a different electronic structure than bulk water.[1] TEY-XAS can though hardly be applied to NDs colloidal dispersions because of the small penetration length of electrons, which makes the method extremely surface sensitive. We previously characterized the electronic structure of NDs in aqueous dispersion by fluorescence yield (FY) XAS and XES.[25] Although this previous study provided new insights on the influence of aqueous dispersion on the surface chemistry of NDs, the water organization around NDs could not be probed because FY-XAS measurements are sensitive to saturation effects, which complicates the interpretation of XA water spectra,[18] and the sensitivity of XES to the hydrogen bond network was not sufficient to reliably estimate the water structure around NDs.[25]

In this communication, aqueous dispersions of NDs with different sizes and surface chemistries are characterized by XAS in pure transmission mode. Transmission measurements are particularly relevant because they do not suffer from saturation artifacts of FY measurements and are sensitive to the whole volume exposed to X-rays, which is adapted to nanoparticle dispersions. Experiments were performed at the UVSOR-III synchrotron facility using a flow cell described elsewhere.[26] Briefly, the liquid sample flows between two 100 nm-thick silicon nitride membranes and is exposed to the soft X-ray beam as shown on Figure 1. The thickness of the probed liquid volume can be controlled down to 20 nm by modifying the helium pressure in the chamber to have an optimal absorbance. The transmitted X-rays are then detected with a photodiode.

Detonation ND aqueous dispersions produced by Plasmachem (NDs-PC, 3−5 nm), International Technology Center (NDs-ITC, 5 nm), and NanoCarbon Research Institute (NDs-

Received: April 21, 2015
Accepted: July 8, 2015
Published: July 8, 2015

DOI: 10.1021/acs.jpclett.5b00820
J. Phys. Chem. Lett. 2015, 6, 2909−2912

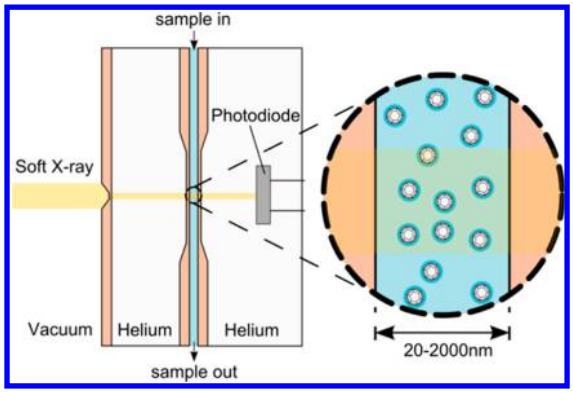

Figure 1. Transmission cell for XAS measurements of aqueous dispersions of NDs.

NRI, 3 nm) were compared to a high-pressure, high-temperature ND aqueous dispersion (NDs-SYP from Van Moppes, 18 nm). The hydrodynamic diameter and the zeta potential (ZP) of NDs in aqueous dispersions characterized in this study are summarized in Supporting Information (SI) Table S1. NDs-SYP and NDs-NRI have hydrodynamic diameter close to their core sizes, therefore these aqueous dispersions are considered monodisperse. On the other hand, NDs-PC and NDs-ITC form small aggregates with sizes up to 32.5 nm, which are probably induced by water dilution performed before size measurement. Furthermore, detonation NDs aggregates have a fractal structure with pores in the nanometer range in which water can diffuse.[17,27] Consequently, we estimate that the extent of the ND−water interface is not significantly affected by slight aggregation of NDs. Except for NDs-NRI, the NDs exhibit negative ZP, which is related to carboxylic groups on their surface.

XAS of the carbon K-edges of the different NDs aqueous dispersions were first measured (Figure S2). The pre-edge region below 289 eV is sensitive to the surface chemistry of NDs. Π* transitions from sp^2-hybridized carbon at 285.0 eV are observed for NDs-NRI but cannot be clearly resolved on other NDs. This feature demonstrates the presence of fullerene-like reconstructions (FLRs) on the surface of NDs-NRI, which may be at the origin of their positive ZP due to oxygen hole doping.[28] On the contrary, the shoulder at 287 eV, which was previously attributed either to FLRs[29] or to C═O bonds,[30] is observed on all NDs except NDs-NRI. Considering that this feature is not observed on NDs-NRI, covered by FLRs as confirmed by the π^* component at 285.0 eV, it can safely be assigned to C═O bonds.

The oxygen K-edges of the different NDs dispersions were then compared to pure water (Figure 2). Typical water XA spectra are constituted of three regions, the pre-edge at 534.7 eV, the main-edge between 537 and 538 eV and the post-edge around 540 eV. The spectra were normalized before the pre-edge and after the post-edge to take into account variations in the sample thickness (see SI). The overall X-ray absorption is higher for NDs dispersions but also differs with the samples. At the main- and post-edges, the absorption coefficient increases for decreasing NDs sizes as discussed later. On the other hand, the intensity of the pre-edge peak at 534.7 eV is stronger for NDs-PC and NDs-ITC, having larger sizes than NDs-NRI (Figure 2).

Changes of X-ray absorption of the oxygen K-edge can be interpreted in terms of modification of the hydrogen bond

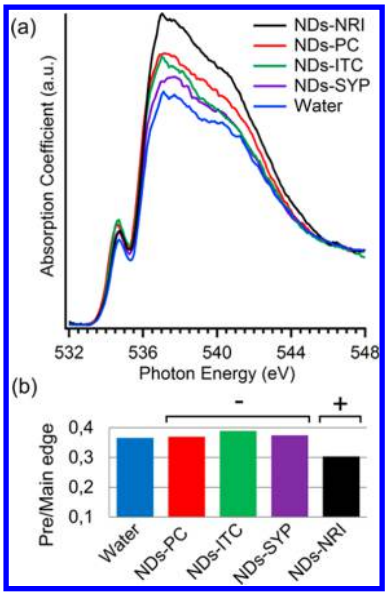

Figure 2. (a) XAS of oxygen K-edge from water and 1% aqueous dispersions of NDs with different origins in transmission cell. (b) Pre/main-edge ratios for the different NDs dispersions. The sign of the NDs ZP in water is indicated above the respective bars.

network in interfacial water layers surrounding dispersed NDs.[18−22] Other explanations for XAS changes are unlikely as discussed in Supporting Information. First, the increased absorption for smaller NDs may be due to higher surface area, increasing the amount of interfacial water molecules. Nevertheless, if the X-ray absorption increase in the main- and post-edges correlates with the respective sizes of the NDs, changes in the pre-edge cannot be simply explained in terms of higher surface area. Indeed, XAS of NDs-NRI, having a higher surface area but a positive ZP, present a smaller pre-edge than other detonation NDs (Figure 2). As a consequence, the surface charge of NDs also has to be taken into account.

A parallel can be performed with a recent report by Velasco-Velez et al. on gold electrodes exposed to electrical bias.[1] The surface potential of the gold electrode was found to strongly influence the XA spectra of interfacial water. In this study, the pre-edge feature was clearly resolved at negative bias, while it fully disappears for positive bias. This was interpreted as a result of orientation of water molecules with their H atoms pointing toward the negatively charged surface, increasing the number of dangling hydrogen bonds at the interface. This is in line with the modifications induced by oxidized NDs observed in the pre-edge region in our case. Carboxylate groups on their surface promote the breaking of hydrogen bonds between water molecules in the first solvation shell. There are thus less water molecules in double hydrogen bond donor configuration, and the pre-edge feature in XAS increases.

On the other hand, positively charged NDs (NDs-NRI) have lower impact in the pre-edge region, probably because the positive surface charges favor orientation of water's oxygen atom toward the surface, leaving both hydrogen atoms available for hydrogen bond formation. Interfacial water molecules donating two hydrogen bonds are promoted, but this molecular orientation does not contribute to the pre-edge region.[1] Hydrogen bonds between neighboring water molecules in the first solvation shell of positively charged NDs are thus promoted compared to negatively charged NDs.

DOI: 10.1021/acs.jpclett.5b00820
J. Phys. Chem. Lett. 2015, 6, 2909−2912

The strong impact of NDs-NRI on the water structure is confirmed by probing the evolution of oxygen K-edge XA spectra at higher NDs concentrations up to 8.6 wt %. As seen in Figure 3, the main- and post-edges increase significantly

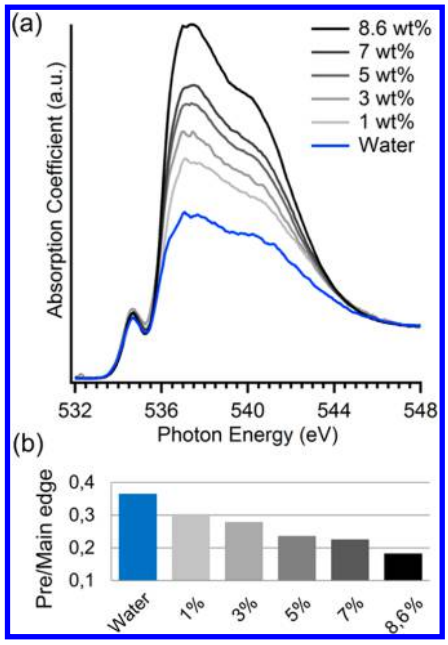

Figure 3. (a) XAS of oxygen K-edge from water and aqueous dispersion of NDs-NRI at different concentrations ranging from 1 to 8.6 wt %. (b) Pre/Main-edge ratios for the different NDs-NRI concentrations.

compared to pure water, while the pre-edge is only slightly perturbed. The X-ray absorption increases in similar amount at main and post edges between 1 and 8.6 wt % NDs concentrations. On the other hand, the pre/main-edge ratio at 8.6 wt % NDs concentration represents only 60% of the same ratio calculated for 1 wt % concentration (Figure 3b). The quenching of the pre-edge in the interfacial water layer surrounding positively charged NDs may result from the orientation of water molecules with oxygen sites pointing toward the NDs surface over several water layers.[1] Due to this arrangement, hydrogen bonds between the hydrogen sites of a water layer with the oxygen site of the next water layer would be stronger than in bulk water, resulting in a higher amount of double donor/double acceptor water molecules, poorly contributing to the pre-edge.

As a result, the increase in main- and post-edges at high concentration of NDs-NRI appears extreme compared to other reports by transmission XAS on aqueous ionic solutions[20] and methanol–water mixtures,[22] although higher mass concentrations were used in these studies. The oxygen K-edge XAS spectra include the contributions of both bulk water and the interfacial water around NDs. By increasing the NDs concentration, the ratio of the interfacial water is increased compared to bulk water, which causes the increase of the main- and post-edges for high NDs concentrations.

Whereas ions mostly perturb water molecules in their first solvation shell,[31] the disruption of the hydrogen bond network induced by small NDs is more extended, apparently over more than four hydration layers according to the strong changes observed on XAS. Unlike ions, NDs are too large to be engulfed in a hydration cage which would break a limited amount of hydrogen bonds.[32] In the same time, they are small enough to offer a large interface and the surface polarization orients water molecules in the first solvation shell. Further investigations are required to estimate whether the long-range order of water molecules around NDs may be correlated to the high viscosity of detonation NDs dispersions at concentration around 8–10 wt %.[13,17]

The electronic structure of interfacial water on NDs can be compared to different forms of ice previously characterized by X-ray Raman scattering.[33,34] Tetrahedral ice and low density amorphous ice present a predominant post-edge structure, related to the less distorted hydrogen bond environment dominated by tetrahedral hydrogen bonds.[33] The electronic signature of high-density amorphous ice,[33,34] on the other hand, is constituted of an intense main-edge and reduced pre- and post-edges, which was attributed to a collapse of the second hydration shell, resulting in higher water molecule density.[20] This electronic signature is close to the one observed around NDs, suggesting that the structure of the ordered water layer around NDs might resemble high density amorphous ice. A similar water structure was observed inside living cells,[35] therefore NDs could potentially be used as a crowding agent to mimic cellular environment.[6]

In summary, the hydrogen bond network of water molecules in aqueous dispersions of NDs was probed by transmission XAS. Orientation of water molecules in the first solvation shell are found to depend on the ZP of NDs. In particular, more hydrogen bonds are broken at the surface of negatively charged NDs due to electrostatic interaction with carboxylate groups while water molecules donating two hydrogen bonds are dominant on positively charged NDs. A long-range ordering of water molecules around NDs is also evidenced. At high NDs concentration, the electronic structure of water molecules is extremely different from bulk water due to the strong contribution from interfacial water layers. The ordering of water molecules on their surface might be comparable to the arrangement of water molecules around proteins, which could potentially explain the high affinity of NDs for protein adsorption[36] or participate to their low cytoxicity.[37]

■ ASSOCIATED CONTENT

Supporting Information

Experimental details, normalization procedure, DLS measurements, transmission XAS of NDs at the carbon K edge, and discussion of XAS interpretation. The Supporting Information is available free of charge on the ACS Publications website at DOI: 10.1021/acs.jpclett.5b00820.

■ AUTHOR INFORMATION

Corresponding Author

* E-mail: tristan.petit@helmholtz-berlin.de.

Author Contributions

The authors declare no competing financial interests.

Notes

The authors declare no competing financial interest.

■ ACKNOWLEDGMENTS

T.P. acknowledges the Alexander von Humboldt Foundation for financial support. H.Y. is a Research Fellow of the Japan Society of Division for the Promotion of Science. E.O. and R. Y. acknowledge partial financial support from G8RI/JSPS. This work is supported by JSPS Grants-in-Aid for Scientific Research

DOI: 10.1021/acs.jpclett.5b00820
J. Phys. Chem. Lett. 2015, 6, 2909–2912

(No. 26248010). We acknowledge the kind support by staff members of the UVSOR-III synchrotron facility.

REFERENCES

(1) Velasco-Velez, J.-J.; Wu, C. H.; Pascal, T. A.; Wan, L. F.; Guo, J.; Prendergast, D.; Salmeron, M. The Structure of Interfacial Water on Gold Electrodes Studied by X-ray Absorption Spectroscopy. *Science* **2014**, *346*, 831−834.

(2) Jena, K. C.; Hore, D. K. Water Structure at Solid Surfaces and its Implications for Biomolecule Adsorption. *Phys. Chem. Chem. Phys.* **2010**, *12*, 14383−404.

(3) Anderson, A.; Ashurst, W. R. Interfacial Water Structure on a Highly Hydroxylated Silica Film. *Langmuir* **2009**, *25*, 11549−54.

(4) Ruffle, S. V.; Michalarias, I.; Li, J.-C.; Ford, R. C. Inelastic Incoherent Neutron Scattering Studies of Water Interacting with Biological Macromolecules. *J. Am. Chem. Soc.* **2002**, *124*, 565−569.

(5) Merzel, F.; Smith, J. C. Is the First Hydration Shell of Lysozyme of Higher Density than Bulk Water? *Proc. Natl. Acad. Sci. U. S. A.* **2002**, *99*, 5378−83.

(6) Ellis, R. J. Macromolecular Crowding: an Important but Neglected Aspect of the Intracellular Environment. *Curr. Opin. Struct. Biol.* **2001**, *11*, 114−119.

(7) Dewan, S.; Yeganeh, M. S.; Borguet, E. Experimental Correlation between Interfacial Water Structure and Mineral Reactivity. *J. Phys. Chem. Lett.* **2013**, *4*, 1977−1982.

(8) Taylor, C. D.; Neurock, M. Theoretical Insights into the Structure and Reactivity of the Aqueous/Metal Interface. *Curr. Opin. Solid State Mater. Sci.* **2005**, *9*, 49−65.

(9) Zobel, M.; Neder, R. B.; Kimber, S. A. J. Universal Solvent Restructuring Induced by Colloidal Nanoparticles. *Science* **2015**, *347*, 292−4.

(10) Spagnoli, D.; Allen, J. P.; Parker, S. C. The Structure and Dynamics of Hydrated and Hydroxylated Magnesium Oxide Nanoparticles. *Langmuir* **2011**, *27*, 1821−9.

(11) Batsanov, S. S.; Lesnikov, E. V.; Dan'kin, D. A.; Balakhanov, D. M. Water Shells of Diamond Nanoparticles in Colloidal Solutions. *Appl. Phys. Lett.* **2014**, *104*, 133105.

(12) Korobov, M. V.; Avramenko, N. V.; Bogachev, A. G.; Rozhkova, N. N.; Osawa, E. Nanophase of Water in Nano-diamond Gel. *J. Phys. Chem. C* **2007**, *111*, 7330−7334.

(13) Ōsawa, E.; Ho, D.; Huang, H.; Korobov, M. V.; Rozhkova, N. N. Consequences of Strong and Diverse Electrostatic Potential Fields on the Surface of Detonation Nanodiamond Particles. *Diamond Relat. Mater.* **2009**, *18*, 904−909.

(14) Dolenko, T. A.; Burikov, S. A.; Rosenholm, J. M.; Shenderova, O. A.; Vlasov, I. I. Diamond−Water Coupling Effects in Raman and Photoluminescence Spectra of Nanodiamond Colloidal Suspensions. *J. Phys. Chem. C* **2012**, *116*, 24314−24319.

(15) Manus, L. M.; Mastarone, D. J.; Waters, E. A.; Zhang, X.-Q.; Schultz-Sikma, E. A.; Macrenaris, K. W.; Ho, D.; Meade, T. J. Gd (III)-Nanodiamond Conjugates for MRI Contrast Enhancement. *Nano Lett.* **2010**, *10*, 484−9.

(16) Ji, S.; Jiang, T.; Xu, K.; Li, S. FTIR Study of the Adsorption of Water on Ultradispersed Diamond Powder Surface. *Appl. Surf. Sci.* **1998**, *133*, 231−238.

(17) Korobov, M. V.; Batuk, M. M.; Avramenko, N. V.; Ivanova, N. I.; Rozhkova, N. N.; Ōsawa, E. Aggregate Structure of "Single-Nano Buckydiamond" in Gel and Dried Powder by Differential Scanning Calorimetry and Nitrogen Adsorption. *Diamond Relat. Mater.* **2010**, *19*, 665−671.

(18) Cappa, C. D.; Smith, J. D.; Messer, B. M.; Cohen, R. C.; Saykally, R. J. Effects of Cations on the Hydrogen Bond Network of Liquid Water: New Results from X-ray Absorption Spectroscopy of Liquid Microjets. *J. Phys. Chem. B* **2006**, *110*, 5301−9.

(19) Aziz, E. F.; Zimina, A.; Freiwald, M.; Eisebitt, S.; Eberhardt, W. Molecular and Electronic Structure in NaCl Electrolytes of Varying Concentration: Identification of Spectral Fingerprints. *J. Chem. Phys.* **2006**, *124*, 114502.

(20) Waluyo, I.; Nordlund, D.; Bergmann, U.; Schlesinger, D.; Pettersson, L. G. M.; Nilsson, A. A Different View of Structure-Making and Structure-Breaking in Alkali Halide Aqueous Solutions through X-ray Absorption Spectroscopy. *J. Chem. Phys.* **2014**, *140*, 244506.

(21) Tokushima, T.; Horikawa, Y.; Takahashi, O.; Arai, H.; Sadakane, K.; Harada, Y.; Takata, Y.; Shin, S. Solvation Dependence of Valence Electronic States of Water Diluted in Organic Solvents Probed by Soft X-ray Spectroscopy. *Phys. Chem. Chem. Phys.* **2014**, *16*, 10753−61.

(22) Nagasaka, M.; Mochizuki, K.; Leloup, V.; Kosugi, N. Local Structures of Methanol−Water Binary Solutions Studied by Soft X-ray Absorption Spectroscopy. *J. Phys. Chem. B* **2014**, *118*, 4388−96.

(23) Lange, K. M.; Könnecke, R.; Soldatov, M.; Golnak, R.; Rubensson, J.-E.; Soldatov, A.; Aziz, E. F. On the Origin of the Hydrogen-Bond-Network Nature of Water: X-Ray Absorption and Emission Spectra of Water−Acetonitrile Mixtures. *Angew. Chem.* **2011**, *123*, 10809−10813.

(24) Petit, T.; Lange, K. M.; Conrad, G.; Yamamoto, K.; Schwanke, C.; Hodeck, K. F.; Dantz, M.; Brandenburg, T.; Suljoti, E.; Aziz, E. F. Probing Ion-Specific Effects on Aqueous Acetate Solutions: Ion Pairing versus Water Structure Modifications. *Struct. Dyn.* **2014**, *1*, 034901.

(25) Petit, T.; Pflüger, M.; Tolksdorf, D.; Xiao, J.; Aziz, E. F. Valence Holes Observed in Nanodiamonds Dispersed in Water. *Nanoscale* **2015**, *7*, 2987−2991.

(26) Nagasaka, M.; Yuzawa, H.; Horigome, T.; Hitchcock, A. P.; Kosugi, N. Electrochemical Reaction of Aqueous Iron Sulfate Solutions Studied by Fe L-edge Soft X-ray Absorption Spectroscopy. *J. Phys. Chem. C* **2013**, *117*, 16343−16348.

(27) Tomchuk, O. V.; Volkov, D. S.; Bulavin, L. A.; Rogachev, A. V.; Proskurnin, M. A.; Korobov, M. V.; Avdeev, M. V. Structural Characteristics of Aqueous Dispersions of Detonation Nanodiamond and Their Aggregate Fractions as Revealed by Small Angle Neutron Scattering. *J. Phys. Chem. C* **2015**, *119*, 794−802.

(28) Petit, T.; Arnault, J.-C.; Girard, H. A.; Sennour, M.; Kang, T.-Y.; Cheng, C.-L.; Bergonzo, P. Oxygen Hole Doping of Nanodiamond. *Nanoscale* **2012**, *4*, 6792−9.

(29) Raty, J.-Y.; Galli, G.; Bostedt, C.; van Buuren, T. W.; Terminello, L. J. Quantum Confinement and Fullerene-like Surface Reconstructions in Nanodiamonds. *Phys. Rev. Lett.* **2003**, *90*, 37401.

(30) Shpilman, Z.; Gouzman, I.; Minton, T. K.; Shen, L.; Stacey, A.; Orwa, J.; Prawer, S.; Cowie, B. C. C.; Hoffman, A. A Near Edge X-Ray Absorption Fine Structure Study of Oxidized Single Crystal and Polycrystalline Diamond Surfaces. *Diamond Relat. Mater.* **2014**, *45*, 20−27.

(31) Omta, A. W.; Kropman, M. F.; Woutersen, S.; Bakker, H. J. Negligible Effect of Ions on the Hydrogen-Bond Structure in Liquid Water. *Science* **2003**, *301*, 347−349.

(32) Chandler, D. Interfaces and the Driving Force of Hydrophobic Assembly. *Nature* **2005**, *437*, 640−7.

(33) Tse, J. S.; Shaw, D. M.; Klug, D. D.; Patchkovskii, S.; Vankó, G.; Monaco, G.; Krisch, M. X-ray Raman Spectroscopic Study of Water in the Condensed Phases. *Phys. Rev. Lett.* **2008**, *100*, 095502.

(34) Pylkkänen, T.; Giordano, V. M.; Chervin, J.-C.; Sakko, A.; Hakala, M.; Soininen, J. A.; Hämäläinen, K.; Monaco, G.; Huotari, S. Role of Non-Hydrogen-Bonded Molecules in the Oxygen K-Edge Spectrum of Ice. *J. Phys. Chem. B* **2010**, *114*, 3804−8.

(35) Ford, R. C.; Ruffle, S. V.; Ramirez-Cuesta, A. J.; Michalarias, I.; Beta, I.; Miller, A.; Li, J. Inelastic Incoherent Neutron Scattering Measurements of Intact Cells and Tissues and Detection of Interfacial Water. *J. Am. Chem. Soc.* **2004**, *126*, 4682−8.

(36) Wang, H.-D.; Niu, C. H.; Yang, Q.; Badea, I. Study on Protein Conformation and Adsorption Behaviors in Nanodiamond Particle−Protein Complexes. *Nanotechnology* **2011**, *22*, 145703.

(37) Paget, V.; Sergent, J. A.; Grall, R.; Altmeyer-Morel, S.; Girard, H. A.; Petit, T.; Gesset, C.; Mermoux, M.; Bergonzo, P.; Arnault, J. C.; et al. Carboxylated Nanodiamonds are neither Cytotoxic nor Genotoxic on Liver, Kidney, Intestine and Lung Human Cell Lines. *Nanotoxicology* **2014**, *8*, 46−56.

DOI: 10.1021/acs.jpclett.5b00820
J. Phys. Chem. Lett. 2015, 6, 2909−2912